



Ion emission spectra in the Jovian X-ray aurora

V. Kharchenko,¹ A. Dalgarno,¹ D. R. Schultz,² and P. C. Stancil³

Received 13 February 2006; revised 4 April 2006; accepted 27 April 2006; published 6 June 2006.

[1] X-ray and Extreme Ultraviolet emission spectra resulting from energetic sulfur and oxygen ions precipitating into the Jovian atmosphere are calculated. Monte Carlo simulations of the energy and charge relaxation of downward ion fluxes are carried out, using updated collision cross sections for stripping, electron capture, and target ionization. Energy and charge distributions of precipitating sulfur ions are presented for the first time and the equilibrium charge model is shown to be inadequate. X-ray emission spectra are calculated for different sulfur and oxygen mixtures and for different initial entry energies. Satisfactory agreement with both Chandra and XMM-Newton observations is obtained by an equal population of sulfur and oxygen ions with energies between 1 and 2 MeV/amu. The agreement provides a reconciliation of the two spectral data sets and the inferred initial energies are consistent with the view that the ions are magnetospheric in origin and have been accelerated to MeV/amu energies. **Citation:** Kharchenko, V., A. Dalgarno, D. R. Schultz, and P. C. Stancil (2006), Ion emission spectra in the Jovian X-ray aurora, *Geophys. Res. Lett.*, 33, L11105, doi:10.1029/2006GL026039.

1. Introduction

[2] The first observations of X-ray emission from the Jovian atmosphere were made in 1979 and 1981 with the Einstein X-ray Observatory [Metzger *et al.*, 1983]. Fluxes of X-ray photons with energies between 0.2 and 3.0 keV were detected from the Jovian North and South poles; this emission defines the Jovian X-ray aurora [Waite *et al.*, 1988]. It was concluded that electron bremsstrahlung was not capable of reproducing the spectra [Metzger *et al.*, 1983]. Later investigations with more advanced X-ray satellite telescopes, ROSAT, Chandra, and XMM-Newton, have added more information on Jovian X-rays [Waite *et al.*, 1994, 1997; Gladstone *et al.*, 2002; Branduardi-Raymont *et al.*, 2004; Bhardwaj *et al.*, 2005]. It was found that the X-rays are characterized by two distinct components, which differ in morphology and in spectra. Two independent sources have been suggested as the origin of the X-ray emissions. The first, the scattering and fluorescence of solar X-rays by the Jovian atmospheric gas, dominates in the equatorial regions [Maurellis *et al.*, 2000]. The second, the auroral X-rays, is emission from the high latitude regions

near the North and South poles. While the intensities and spectral characteristics of the equatorial X-rays are satisfactorily described by the fluorescence mechanism, the nature of the Jovian auroral X-rays is still uncertain.

[3] A detailed analysis of electron bremsstrahlung emission as a source of the Jovian X-ray aurora has been carried out by Barbosa [1992], who calculated the flux of energetic electrons, required for production of the observed X-ray intensities. This electron flux would yield unrealistically high power of the Jovian UV/EUV aurora [Waite *et al.*, 1992; Cravens *et al.*, 2003]. In recent observations of Jovian X-rays with the Chandra [Gladstone *et al.*, 2002; Elsner *et al.*, 2005] and XMM-Newton [Branduardi-Raymont *et al.*, 2004] the spectral resolution has been significantly improved in comparison with the ROSAT and Einstein data, and distinct spectral features were detected. The bremsstrahlung mechanism is not capable of explaining the non-monotonic behavior of the X-ray spectra as a function of photon energy.

[4] A heavy-ion aurora has been suggested as an alternative mechanism [Metzger *et al.*, 1983]. With it, X-rays are produced by precipitating energetic oxygen and sulfur ions, originating from the Io torus. The initial flux of low-charged ions [Gehrels and Stone, 1983] is transformed into a flux of highly-charged particles by sequential ion stripping collisions with atoms and molecules of the Jovian atmospheric H, H₂, and He. Highly stripped O^{q+} and S^{q+} ions induce X-ray and EUV emission in charge-exchange (CX) collisions with the atmospheric gas. The spectra and strength of the X-ray emission depend on the intensity, initial energy, and elemental composition of the precipitating ions.

[5] Observations with the Chandra telescope provided a more complete view of the morphology of the X-ray auroras. Regions of X-ray emissions from the South and North poles were found to narrow near the polar caps, indicating that the precipitating heavy ions enter the atmosphere from distances larger than 30 Jovian radii and heavy ions cannot be picked up from the Io torus [Cravens *et al.*, 2003]. The initial ion kinetic energies must be about 2 MeV/amu, higher than the energy of ~0.5 MeV/amu inferred from the ROSAT data. Other mechanisms that produce fluxes of energetic ions in Jovian polar regions, have been discussed by Cravens *et al.* [2003]. They showed that the heavy solar wind and outer magnetospheric ions, if they are accelerated along magnetic field lines up to energies of 1–2 MeV/amu, produce X-rays with the power and morphology of the Jovian X-ray auroras. X-ray emission features of the Jovian auroras have been detected with Chandra [Gladstone *et al.*, 2002; Elsner *et al.*, 2005] and with XMM-Newton [Branduardi-Raymont *et al.*, 2004], and calculations of the spectra, resulting from charge-exchange of oxygen ions, have been carried out [Horanayi *et al.*, 1988; Cravens *et al.*, 1995; Kharchenko *et al.*, 1998; Liu and Schultz, 1999]. The contribution from energetic sulfur

¹Harvard-Smithsonian Center for Astrophysics, Cambridge, Massachusetts, USA.

²Oak Ridge National Laboratory, Oak Ridge, Tennessee, USA.

³Department of Physics and Astronomy and Center for Simulational Physics, University of Georgia, Athens, Georgia, USA.

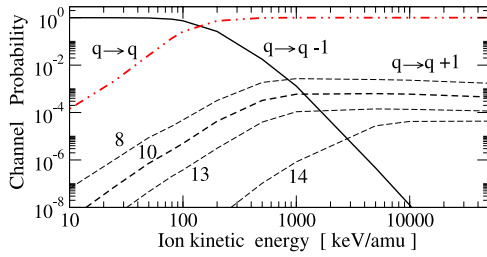


Figure 1. The probabilities of the different collisional channels as functions of the kinetic energy of S^{10+} ions in collisions with H_2 . Stripping probability is shown by the dashed curve, and the charge-exchange and target-ionization probabilities by the solid and dot-dashed curves respectively. Stripping probabilities are shown also for $q = 8, 13$ and 14 sulfur ions.

ions was obtained by a simple scaling of the oxygen results. There are significant differences between the observations and the theoretical results. Here we employ a set of reliable sulfur ion cross sections and we predict the X-ray spectra produced by a mixture of oxygen and sulfur ions precipitating into the Jovian atmosphere and undergoing charge-exchange and ionizing collisions.

2. Energy and Charge Relaxation of Precipitating Ions

[6] Several processes are incorporated into the CX mechanism of X-ray auroras, including the acceleration of magnetospheric and solar wind ions, ion collisions with the Jovian atmospheric gas, and emission of cascading photons by excited ions. We calculate the ion-charge q and energy ϵ distributions in the precipitating ion flux. Distribution functions $f_i(q, \epsilon, n)$ of oxygen $i = O$ and sulfur $i = S$ ions are obtained as functions of the number n of ion collisions with the atoms and molecules of the atmospheric gas. These distributions, which are normalized to a single precipitating ion by the condition $\int d\epsilon \sum_q f_i(q, \epsilon, n) = 1$, allow the calculation of spectra and intensity of X-ray emissions induced independently by O and S ion fluxes [Cravens *et al.*, 1995; Kharchenko *et al.*, 1998; Liu and Schultz, 1999; Cravens *et al.*, 2003]. Initial kinetic energies of precipitating ions at the top of the Jovian atmosphere were chosen between 0.5 and 2 MeV/amu, consistent with the acceleration mechanism discussed by Cravens *et al.* [2003]. Collisions of the fast ions i^{q+} with the atmospheric gas lead to the energy degradation of the precipitating flux. Some of the collisional channels, such as the target ionization collisions, reduce the ion kinetic energy ϵ , and do not influence the ion charge q . The energetic ions may change their charge states due to electron capture or electron loss in collisions with H and He atoms and H_2 molecules. At high ion energies, the probability of stripping collisions $q \rightarrow q + 1$ is much larger than the charge-exchange $q \rightarrow q - 1$ probability. Stripping collisions induce a rapid increase in the average charge of ions in the precipitating flux for initial ion energies of order MeV/amu. At such high energies, the probability of energy loss collisions without q -changing is larger by 3–4 orders of magnitude than the probabilities of the $q \pm 1$ channels: thousands of energy loss collisions $q \rightarrow$

q happen before any charge changes. The rates of the energy relaxation of precipitating ions at MeV/amu energies are much larger than the charge relaxation rate, and equilibrium charge distributions, for which the loss of ions in any charge state is exactly compensated by their production [Kharchenko *et al.*, 1995], are never established [Kharchenko *et al.*, 1998].

[7] Stripping collisions create a population of highly charged ions O^{q+} ($q \sim 5-8$) and S^{q+} ($q \sim 8-14$), which produce highly excited ions in the electron-capture process. Excited highly-charged ions radiate X-ray and EUV photons [Metzger *et al.*, 1983; Cravens *et al.*, 1995; Kharchenko *et al.*, 1998]. We consider three channels that alter the ion charge states in the elementary collision $i^{q+} \rightarrow i^{q'++}$, where q and $q' = q, q \pm 1$ are the ion charges before and after collision. The channel probabilities $p_i(q, q', \epsilon)$ of the “ i ”-th ion depend on the collision energy ϵ and ion charge q . We have calculated channel probabilities for the oxygen and sulfur ions in the energy interval of 0.01–5 MeV/amu, using ratios of the channel cross sections $\sigma_i(q, q', \epsilon)$ to the total cross section $\sigma_i(\epsilon)$: $p_i(q, q', \epsilon) = \sigma_i(q, q', \epsilon) / \sigma_i(\epsilon)$. Detailed information on O^{q+} and S^{q+} cross sections and channel probabilities for collisions with H_2 will be published separately (D. R. Schultz *et al.*, manuscript in preparation, 2006). Cross sections for H and He were obtained from the H_2 data by using the appropriate mass for the target and assuming the cross sections are functions of ϵ/I , where I is the ionization potential of the target atom. We show in Figure 1 the probabilities of the charge-exchange, stripping, and target ionization/excitation channels for collisions of S^{10+} ions with H_2 molecules. The stripping probability is larger than that for charge-exchange at energies above 1 MeV/amu, and the probability of the energy loss collisions $q \rightarrow q$ (dot-dashed curve in Figure 1) dominates by four orders of magnitude with respect to other channels. Because of efficient energy loss, the equilibrium charge distribution, defined as the ion-charge distribution at a fixed kinetic energy of the precipitating flux, cannot be reached [Kharchenko *et al.*, 1998]. As ions slow down in collisions with atmospheric gas, electron capture collisions become a dominant channel, and the average ion charge decreases. Low charge ions do not produce X-rays and emit only UV and EUV photons. The average charge $\langle q \rangle = \int d\epsilon \sum_q q f_i(q, \epsilon, n)$ of energetic sulfur ions, propagating in an H_2 gas, is presented in Figure 2 as a function of the average ion energy $\langle \epsilon \rangle = \int d\epsilon \sum_q \epsilon f_i(q, \epsilon, n)$. We calculated

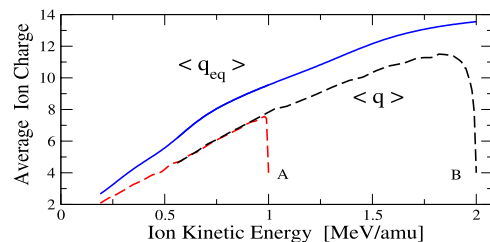


Figure 2. Dependence of the average ion charge $\langle q \rangle$ on the average kinetic energy ϵ of precipitating S ions. The dashed curves A and B describe the evolution of the ion average charge as function of the average kinetic energy of S ions, precipitating with the initial energies 1 and 2 MeV/amu respectively. Solid curve is the average ion charge determined from the equilibrium-charge model.

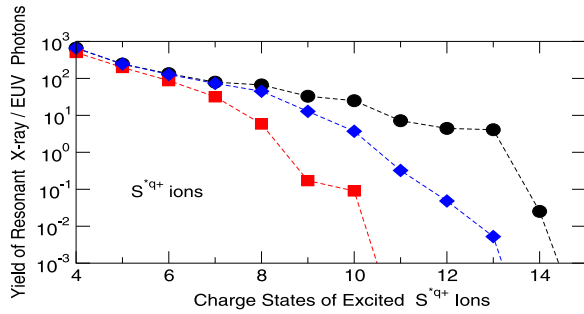


Figure 3. Yield of the resonant X-ray and EUV photons from the different charge states of the excited sulfur S^{*q+} ions. The number of photons is normalized per single precipitating ion. Squares, diamonds, and circles show the photon yield at initial ion energies of 0.7, 1, and 2 MeV/amu. To guide the reader, the numbers of photons induced from the different q -states are connected by dashed lines.

the dependence of $\langle q \rangle$ on $\langle \epsilon \rangle$ using Monte Carlo simulations of the propagation of initially low-charged and highly-energetic S^{3+} ions in H_2 . Stripping in the initial stage leads to a sharp increase of the average ion charge $\langle q \rangle \sim 7.5$ and 11.5 for sulfur ions entering with initial energies of 1 MeV/amu and 2 MeV/amu respectively. As the average kinetic energy of the ion beam decreases, a gradual reduction of the average charge occurs, and as shown in Figure 2 by the solid curve, the $\langle q \rangle$ -charge never reaches the equilibrium value. The inequality of the dynamical and equilibrium $\langle q \rangle$ charges reflects the difference between charge and energy relaxation rates [Kharchenko *et al.*, 1998]. The total yield of X-ray photons and their spectra are especially sensitive to the highly-charged fraction of the ion charge distribution.

3. Yield of X-Ray Photons

[8] The yields of X-ray photons in the Jovian auroras are calculated from the ion energy-charge distributions in the downward O^{q+} and S^{q+} fluxes, using the method described by Cravens *et al.* [1995] and Kharchenko *et al.* [1998]. We report for the first time the results of accurate calculations of energy-charge distributions, X-ray and EUV yields, and X-ray emission spectra of sulfur ions precipitating into the Jovian atmosphere using new cross sections for collisions of S^{q+} ions with H_2 molecules and improved cross sections of O^{q+} ions. To evaluate the ion energy-charge distributions for the entire precipitation process, we employed the Monte Carlo method [Kharchenko *et al.*, 1998], and considered magnetospheric O^{q+} and S^{q+} ions with initial precipitation energies of 0.5–2 MeV/amu. Distributions $f_i(q, \epsilon, n)$ have been constructed from Monte Carlo simulations of the propagation of ensembles of monoenergetic particles, which include 10^4 – 10^5 initially low-charge $q \sim 1$ –3 ions with kinetic energies ϵ in the range 0.5–2 MeV/amu. The stopping of energetic ions requires 10^5 – 10^6 collisions, and highly charged ions lose and capture electrons several times. Every capture leads to the emission of at least one X-ray photon, and for the entire stopping process an energetic ion may radiate more than a hundred X-ray photons with energies larger than 0.1 keV. The photon yield, defined as the number of X-ray and EUV photons

emitted in resonant transitions during the entire energy relaxation event by excited S^{*q+} ($q = 4$ –15) ions, is shown in Figure 3 for sulfur ions precipitating with initial energies of 0.7, 1, and 2 MeV/amu. Low charge state ions with $q = 4$ or 5 induce only EUV photons with energies of 60–70 eV. The initial charge state of the precipitating ion does not influence the quantum yield because of the efficient stripping of the ion on entry into the atmosphere. The low charge states produce orders of magnitude more photons than do high-charge states. For example, at the initial ion energy of 0.7 MeV/amu about a hundred X-ray photons with energies between 274 and 400 eV. Emission from charge states higher than 10 is absent from ions with an initial energy of 0.7 MeV/amu, because a 0.7 MeV/amu projectile does not strip ions to highly charged states. At higher initial energies, the fractions of highly stripped ions and energetic photons are increased. For S^{q+} with an initial energy of 2 MeV/amu, the most energetic X-ray photons with energies of 2.43–3.16 keV are induced by S^{*14+} ions, but the yield of these photons is very small at about 0.03 photons per precipitating sulfur ion.

[9] We have computed X-ray spectra induced by mixtures of the precipitating oxygen and sulfur ions, using the photon yield functions for different initial energies of O^{q+} and S^{q+} .

4. Comparison Between Theory and Observations

[10] Our predictions for the charge-exchange model are compared with the Jovian X-rays detected in the Chandra [Elsner *et al.*, 2005] and XMM-Newton [Branduardi-Raymont *et al.*, 2004] X-ray telescope observations in Figure 4. Approximately equal abundances of energetic O and S ions in the Jovian magnetosphere have been measured with the Galileo and Cassini spacecrafts [Mauk *et al.*, 2004], and the theoretical curves were calculated, assuming an

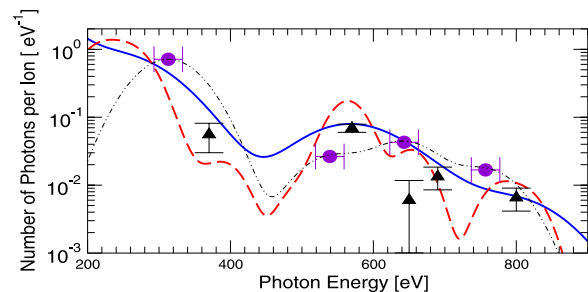


Figure 4. The comparison between the theoretical spectra induced by precipitating S and O ions and the observations of the Jovian northern aurora with the Chandra and XMM-Newton X-ray telescopes. Theoretical spectra are normalized per single precipitating ion. Spectra, computed for photon energy resolutions of 110 and 55 eV, are shown by solid and dashed curves. Circles and triangles are the best-fit spectral features inferred from the Chandra [Elsner *et al.*, 2005] and XMM-Newton [Branduardi-Raymont *et al.*, 2004] observations. The dotted line represents the Gaussian best fit spectra for Chandra observations.

equal fraction of oxygen and sulfur ions precipitating into the Jovian atmosphere. An initial kinetic energy of 1 MeV/amu was assigned to 50% of the oxygen ions and 80% of the sulfur ions. For the rest of the ion population, 2 MeV/amu was chosen as the ion energy at the top of the Jovian atmosphere. The CX spectra, computed for the two photon energy resolutions of 110 and 55 eV, are illustrated by solid and dashed curves. The spectra, detected by the Chandra X-ray telescope from the North pole [Elsner *et al.*, 2005], may be reproduced by four Gaussian lines at 313, 539, 643, and 757 eV with the best-fit intensities shown in Figure 4 by circles. The spectral data from the observations with XMM-Newton yield five lines with photon energies between 370 and 800 eV and intensities shown in Figure 4 by triangles [Branduardi-Raymont *et al.*, 2004]. As shown in Figure 4 the simple composition we adopted for the precipitating flux provides reasonably good agreement between the theoretical curve and both sets of the observational data.

[11] The difference between the XMM-Newton and Chandra spectra is significant at low X-ray energies between 300–400 eV, though the interpretation of the X-ray data is complicated due to the low efficiency of X-ray detection and the limited energy resolution of the measurements [Branduardi-Raymont *et al.*, 2004; Elsner *et al.*, 2005]. Nevertheless, comparison with the theoretical curves, shown in Figure 4, provides a plausible reconciliation of the two sets of observational data. At the low resolution of 110 eV (solid curve), both assignments for the spectral features at 313 eV [Elsner *et al.*, 2005] and 370 eV [Branduardi-Raymont *et al.*, 2004] agree well with the theoretical predictions. Sharp variations of the spectra in the region of 300–400 eV, shown by the theoretical curves in Figure 4, may explain the relative intensities of the spectral features at 313 eV and 370 eV observed with the Chandra and XMM-Newton telescopes [Branduardi-Raymont *et al.*, 2004; Elsner *et al.*, 2005]. X-ray photons induced by S^{q+} and O^{q+} ions below photon energies of 500 eV provide a good description of the soft X-ray emission detected by both telescopes, and the presence of ions of other elements is not necessary for our model. We conclude from Figure 4 that the theoretical spectra at a resolution of 55 eV provide a satisfactory description of the spectral features in the entire set of observational data. The success of the theoretical model lends support to the hypothesis by Cravens *et al.* [2003], that the ions are magnetospheric ions originating at a distance of 30 Jovian radii from the planet and accelerated to energies between 0.5 and 2 MeV/amu.

5. Conclusions

[12] We have identified new features of the CX mechanism obtained in accurate modeling of the charge and energy distributions of the precipitating S^{q+} and O^{q+} ions, using accurate cross sections of the stripping, charge-exchange, and target ionization collisions. We found that for initial energies between 1 and 2 MeV/amu the yield of X-ray photons with energies greater than 250 eV is equal to 73 photons per precipitating ion, which is about 7 times higher than the photon yield obtained for the mixture of S and O ions by scaling the oxygen ion yield [Cravens *et al.*, 1995, 2003; Kharchenko *et al.*, 1998]. We have calculated the emission spectra of the precipitating S and O ions and determined the ion flux composition and initial energies that

yield a spectrum which agrees well with that observed recently with the Chandra and XMM-Newton telescopes. The initial ion energies of 1–2 MeV/amu are in good agreement with the predictions by Cravens *et al.* [2003]. The emission efficiency of the charge-exchange mechanism, defined as the ratio of the intensity of outgoing X-ray photons to the energy of the incoming ion flux, is calculated to be 1.4×10^{-3} . We have derived the absolute density of the precipitating ion flux at the top of the Jovian atmosphere, 2.4×10^5 ions $\text{cm}^{-2}\text{s}^{-1}$, by scaling the normalized theoretical spectra to the Jovian X-ray photon fluxes measured by Chandra and XMM-Newton telescopes from the North pole. The value of the inferred ion flux depends on the initial ion composition and energies, and the area of precipitation, which was estimated as 10^8 km^2 [Cravens *et al.*, 2003]. We determined the absolute flux to be 4–5 times smaller than previous estimates by Cravens *et al.* [2003]. The difference may be explained by the presence of the sulfur ions, which have a yield of soft X-ray photons higher by a factor of 7 than the yield adopted by Cravens *et al.* [2003]. Our calculations support the view that the precipitating ions are magnetospheric ions that have been accelerated.

[13] **Acknowledgments.** This work has been supported by NASA grants NNG04GD57G, NAG5-11453 and NASA contracts W19318 and W19540. We thank T. Cravens for useful discussions of the Jovian X-ray aurora mechanism.

References

- Barbosa, D. D. (1992), Heavy ion dynamics and auroral arc formation in the Jovian magnetosphere, *Adv. Space Res.*, *12*, 7.
- Bhardwaj, A., G. Branduardi-Raymont, R. F. Elsner, G. R. Gladstone, G. Ramsay, P. Rodriguez, R. Soria, J. H. Waite Jr., and T. E. Cravens (2005), Solar control on Jupiter's equatorial X-ray emissions: 26–29 November 2003 XMM-Newton observation, *Geophys. Res. Lett.*, *32*, L03S08, doi:10.1029/2004GL021497.
- Branduardi-Raymont, G., *et al.* (2004), First observation of Jupiter by XMM-Newton, *Astron. Astrophys.*, *424*, 321.
- Cravens, T. E., *et al.* (1995), Auroral oxygen precipitation at Jupiter, *J. Geophys. Res.*, *100*, 17,153.
- Cravens, T. E., *et al.* (2003), Implications of Jovian X-ray emission for magnetosphere-ionosphere coupling, *J. Geophys. Res.*, *108*(A12), 1465, doi:10.1029/2003JA010050.
- Elsner, R. F., *et al.* (2005), Simultaneous Chandra X ray, Hubble Space Telescope ultraviolet, and Ulysses radio observations of Jupiter's aurora, *J. Geophys. Res.*, *110*, A01207, doi:10.1029/2004JA010717.
- Gehrels, N., and E. C. Stone (1983), Energetic oxygen and sulfur ions in the Jovian magnetosphere and their contribution to the auroral excitation, *J. Geophys. Res.*, *88*, 5537.
- Gladstone, G. R., *et al.* (2002), A pulsating auroral X-ray hot spot on Jupiter, *Nature*, *415*, 1000.
- Horanayi, M., T. E. Cravens, and J. H. Waite (1988), The precipitation of energetic heavy ions into the upper atmosphere of Jupiter, *J. Geophys. Res.*, *93*, 7251.
- Kharchenko, V., W. H. Liu, and A. Dalgarno (1998), X ray and EUV emission spectra of oxygen ions precipitating into the Jovian atmosphere, *J. Geophys. Res.*, *103*, 26,687.
- Liu, W. H., and D. R. Schultz (1999), Jovian X-ray aurora and energetic oxygen ion precipitation, *Astrophys. J.*, *526*, 538.
- Mauk, B. H., D. G. Mitchell, R. W. McEntire, C. P. Paranicas, E. C. Roelof, D. J. Williams, S. M. Krimigis, and A. Lagg (2004), Energetic ion characteristics and neutral gas interactions in Jupiter's magnetosphere, *J. Geophys. Res.*, *109*, A09S12, doi:10.1029/2003JA010270.
- Maurellis, A. N., *et al.* (2000), Jovian X-ray emission from solar X-ray scattering, *Geophys. Res. Lett.*, *27*, 1339.
- Metzger, A. E., *et al.* (1983), The detection of X-rays from Jupiter, *J. Geophys. Res.*, *88*, 7731.
- Waite, J. H., J. T. Clarke, T. E. Cravens, and C. M. Hammond (1988), The Jovian aurora: Electron or ion precipitation?, *J. Geophys. Res.*, *93*, 7244.
- Waite, J. H., *et al.* (1992), Jovian bremsstrahlung X-rays—A Ulysses prediction, *Geophys. Res. Lett.*, *19*, 83.
- Waite, J. H., *et al.* (1994), ROSAT observations of the Jupiter aurora, *J. Geophys. Res.*, *99*, 14,799.

Waite, J. H., et al. (1997), Equatorial X-ray emissions: Implications for Jupiter's high exospheric temperatures, *Science*, 276, 104.

A. Dalgarno and V. Kharchenko, Harvard-Smithsonian Center for Astrophysics, Cambridge, MA 02138, USA. (vkharchenko@cfa.harvard.edu)

D. R. Schultz, Oak Ridge National Laboratory, Oak Ridge, TN 37831, USA.

P. C. Stancil, Department of Physics and Astronomy and Center for Simulational Physics, University of Georgia, Athens, GA 30602, USA.